

Development and Comparative Study on Tire Models in the AutoDyn7 Program

DongHoon Han*, JeongHyun Sohn

Graduate School of Mechanical Design and Production Engineering, Pusan National University

KwangSuk Kim

Inha Technical College

JongNyun Lee

Dogseo University

WanSuk Yoo, ByunHoon Lee, JaeWeon Choi

Department of Mechanical Engineering, Pusan National University

In this paper, several tire models (Magic formula, Carpet plot, UA tire, DADS tire and STI tire) are implemented and compared. Since the STI (System Technology Inc.) tire model in the AutoDyn7 program is in a good agreement to NADSdyna STI tire model and experiment, it is selected as a reference tire model for the comparison. To compare tire models, input parameters of each tire model are extracted from the STI tire model to preserve the same tire properties. Several simulations are carried out to compare performances of tire models, i. e., bump simulation, lane change simulation, and pulse steering simulation. The performances in vehicle maneuverability are also compared with the four parameter evaluation method.

Key Words : Tire Model, AutoDyn7, Vehicle Dynamics, Four Parameter Evaluation Method

1. Introduction

Tire has been remarkably improved technologically since the first pneumatic tire was made in 1888 by J. E. Dunlop. As a component of vehicle, tire plays an important role in supporting the vertical load while cushioning against road shocks from surface irregularities. It also endures longitudinal forces for acceleration and braking, and lateral forces for cornering. The properties of tire forces, which is developed in the tire-road contact patch, mainly influence the ride and handling performance with the exception of aerodynamic forces. So, it is important in vehicle

dynamic analysis to choose proper tire model which corresponds to real phenomena.

Bradly and Allen started the study of the dynamic properties of automobiles in 1930s. The first theoretical study on the fundamentals of cornering properties of a tire was performed by Fiala(1954). Bernard et al. (1977) developed a semi empirical-model of the tire used for combined slips. Dugoff et al. (1970) expressed the tire-road friction coefficient as a function of the sliding velocity of the tire tread. Pacejka(1979) proposed a static non-linear tire model, which is named "Magic Formula". Gim et al. (1990) developed an analytical model for vehicle dynamic simulations with the requirement of a minimum input data.

In this paper, characteristics of tire models which used in AutoDyn7 (Automobile Dynamic analysis program developed in G7 project) are compared and analyzed.

* Corresponding Author,

E-mail : handong@web.pusan.ac.kr

TEL : +82-51-510-1457 ; FAX : +82-51-581-8514

Graduate School of Mechanical Design and Production Engineering, Pusan National University, San 30 Jangjun-dong, Kumjung-ku, Pusan 609-735, Korea. (Manuscript Received October 25, 1999; Revised May 12, 2000)

2. Tire Models and Theories

Tire models used in vehicle dynamics analysis can be classified largely into theoretical models and empirical models. In the theoretical model, forces and moments are mathematically described by the tire structure and deformation mechanism, and their equations are rather complex.

The empirical model, however, obtains tire forces and moments from test data for various velocities, slip angles, camber angles, and normal forces. Although an empirical model well describes real phenomena of the tire, it requires time and effort to develop for each type of tires.

In the AutoDyn7 program, five different tire models are developed, i. e., AT_S (AutoDyn7 STI tire model), AT_C (AutoDyn7 Carpet plot), AT_M (AutoDyn7 Magic Formula tire model), AT_D (AutoDyn7 DADS tire model), and AT_A (AutoDyn7 ADAMS UA tire model).

2.1 AT_C (AutoDyn7 Carpet Plot) tire model (Kim et al., 1999)

Carpet plot model computes tire forces and moments from empirical data measured by changing slip angle, camber angle, and normal force during pure cornering and pure braking. To obtain values between measured data, interpolation is usually employed. So, it requires many test data to obtain accurate values. In this model, tire forces and moments have large errors if the input values are out of range of measured data. Table 1 (Choi, 1999) shows an example of experimental conditions to get a carpet plot data. Tests are

Table 1 Experimental condition of tire

Tire type	P195/70R14
Velocity	48.28 km/h (30 mile/h)
Inflation Pressure	30 (psi)
Normal Force	200, 600, 1000, 1400, 1750 (lb)
Camber angle	-10, -6, -2, 0, 2, 6, 10 (deg)
Slip angle	-20, -16, -12, -8, -4, -2, -1, 0 1 2 4 8 12 16 20 (deg)

carried out for total 525 cases ($15 \times 7 \times 5$) with 15 slip angles, 7 camber angles, 5 normal forces.

2.2 AT_M (AutoDyn7 Magic Formula) tire model (Choi, 1999)

AT_M tire model computes tire forces and moments with mathematical relationship from experimental data. It is possible to determine tire forces and moments if desired function is determined in any condition of vehicle. In Eqs. (1) ~ (3) for this formula, the output (Y) represents one of side force, self aligning torque, or brake force. The input (X) denotes the slip angle or the longitudinal slip.

$$x = X + S_x \quad (1)$$

$$y(x) = D \sin [C \tan^{-1} (Bx - E (Bx - \tan^{-1} (Bx)))] \quad (2)$$

$$Y(X) = y(x) + S_y \quad (3)$$

where, B , C , D , E , S_x and S_y are stiffness, shape factor, peak factor, curvature factor, horizontal shift and vertical shift, respectively. If X is the longitudinal slip, Y is the longitudinal force and if X is the slip angle, Y is the lateral force or the self aligning torque. Although the same equations are used, different coefficients are assigned for each case.

2.3 AT_S (AutoDyn7 STI) tire model (Salani, 1996)

When one of the tires forward velocity V_x approaches near zero, the longitudinal and the lateral slip ratios approach infinity which may cause difficulties in the calculation of tire forces. To avoid this problem, Bernard et al (1977) recently formulated the longitudinal and lateral slip ratios as state variables rather than kinematic functions of wheel spin rate and wheel velocity. Their idea was written as the following equations:

$$\dot{k} + \frac{|V_x|}{B} k = \frac{|V_x| - r \theta \text{sign}(V_x)}{B} \quad (4)$$

$$\frac{\partial \tan(\alpha)}{\partial t} + \frac{|V_x|}{b} \tan(\alpha) = \frac{V_y}{b} \quad (5)$$

where B and b are relaxation lengths.

AT_S tire model computes composite slip as in Eq. (6).

$$\sigma = \frac{\pi a_p^2}{8 F_z} \sqrt{\frac{K_s^2 \tan^2 \alpha}{\mu_{py}^2} + \frac{K_c^2}{\mu_{px}^2} \left(\frac{k}{1-k} \right)^2} \quad (6)$$

where a_p , F_z , K_s , K_c , μ_{px} , μ_{py} , k , and α are contact patch length, normal load, longitudinal stiffness, lateral stiffness, peak longitudinal coefficient of friction, peak lateral coefficient of friction, longitudinal slip, and lateral slip, respectively. Also, the force saturation function is computed using the following empirical formula Eq. (7):

$$f(\sigma) = \frac{C_1 \sigma^3 + C_2 \sigma^2 + C_5 \sigma}{C_1 \sigma^3 + C_3 \sigma^2 + C_4 \sigma + 1} \quad (7)$$

where, C_1 , C_2 , C_3 , C_4 and C_5 are shaping parameters.

In the total lateral force equation shown in Eq. (8), the first term produces lateral forces due to the longitudinal and lateral slip, and the second term is due to camber effect.

$$F_y = -\mu_y F_z \frac{f(\sigma) K_s \tan \alpha}{\sqrt{K_s^2 \tan^2 \alpha + K_c^2 k^2}} + Y_\gamma \gamma. \quad (8)$$

The longitudinal force is,

$$F_x = -\mu_x F_z \frac{f(\sigma) K_c k}{\sqrt{K_s^2 \tan^2 \alpha + K_c^2 k^2}}. \quad (9)$$

The aligning moment is computed as follows:

$$M_z = \frac{K_m a_p^2 \tan \alpha}{(1 + G_1 \sigma^2)^2} \left[\frac{K_s}{2} - G_2 K_c \frac{k}{1-k} (2 + \sigma^2) \right] + Y_\gamma \gamma (1 - f(\sigma)) \frac{F_x}{a_p K_s}. \quad (10)$$

2.4 AT_D (AutoDyn7 DADS) tire model (1997)

AT_D tire model, which is similar to the tire model in the DADS program, allows three levels of complexity-simple force model (Type "BASIC"), intermediate force model (Type "INTERMEDIATE"), and the most detailed force model (Type "FULL"). Longitudinal force is computed as a function of the normal force and the friction coefficient depending on the rotational slip. Steering angle and camber angle are computed in the program. If carpet plot data is available, lateral force is computed with the carpet plot model. If not, the constant force curves are approximated by a cubic polynomial determined from the boundary conditions or the lateral spring-damper model.

2.5 AT_A (AutoDyn7 ADAMS UA) tire model (Lee, 1997)

AT_A tire model is developed under the following assumptions, i. e., the contact patch is rectangular, the contact pressure distribution is parabolic over the contact patch width, and tire tread is a beam resting on an elastic foundation. Since friction ellipse concept may produce undesirable results due to equations depending on integration step, friction circle concept is employed. Stiffness is assumed to be a constant. In computing the longitudinal force, contact patch is divided into the sliding region and the adhesion region at circumferential directions. The longitudinal forces are computed by integrating the longitudinal elastic stress in the adhesion region and the frictional stress in the sliding region.

3. Comparison of Tire Models

3.1 Selection of a reference model

AT_S model is compared with the results of NADSDyna (Salaani, 1996) to compare the accuracy and it is selected as a reference tire model. Vehicle model and tire parameters are chosen to be identical to the NADSDyna model. Figure 1 shows step steering input of NADSDyna at the speed of 33m/s. Yaw rate and lateral acceleration are compared in Figs. 2 and 3, respectively. AT_S model is almost the same as NADSDyna model, and those results are in a good agreement to the experiment.

Figure 4 shows pulse steering input at the speed of 23 m/s. Yaw rate and lateral acceleration is compared in Figs. 5 and 6, respectively. The

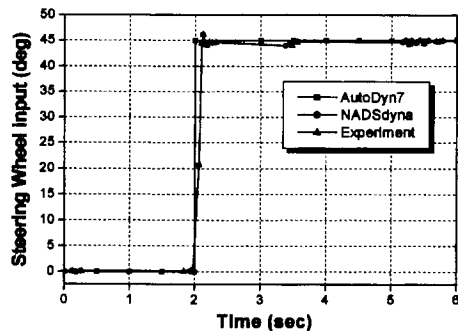


Fig. 1 Step steering input

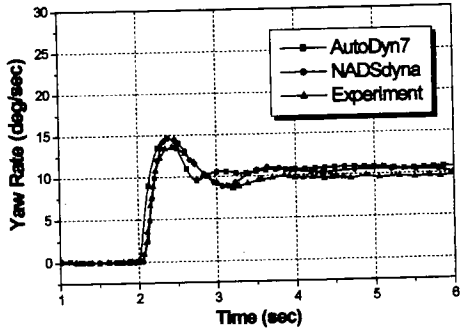


Fig. 2 Yaw Rate of chassis

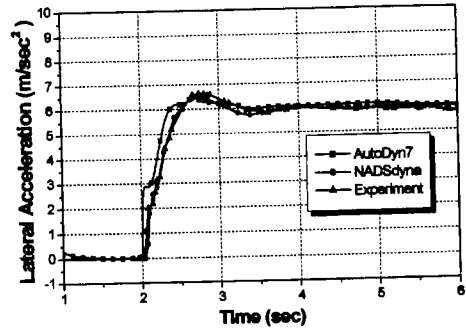


Fig. 3 Lateral acceleration of chassis

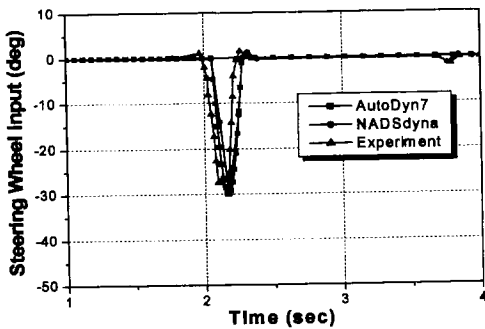


Fig. 4 Pulse steering input

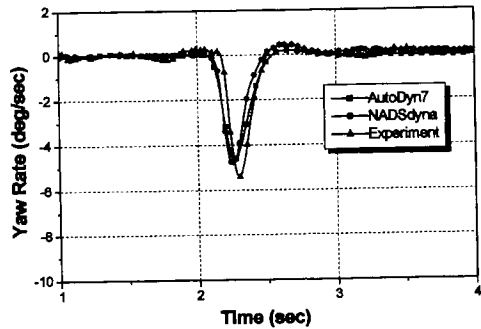


Fig. 5 Yaw rate of chassis

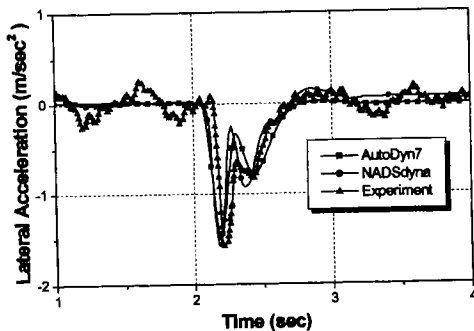


Fig. 6 Lateral acceleration of chassis

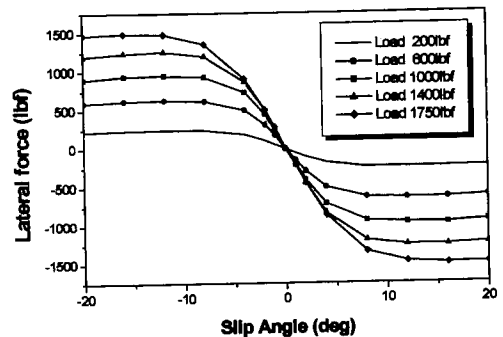


Fig. 7 Lateral Force vs slip

results of AT_S model in pulse steering are also in a good agreement to the NADSdyna and experiment.

Since the AT_S tire model matches well with the experimental results and NADSdyna both in step steering and pulse steering, the AT_S model is selected as a reference model and other tire models are compared to it.

3.2 Determination of tire inputs

Since input parameters are different from each

tire model, it is necessary to adjust the input parameters to have same properties. The input parameters for AT_M tire is derived from curve fitting of the carpet plot and used the results of preceeding research (Paceika, 1979). Stiffness parameters of the AT_D and AT_A, which are theoretical models, are drawn from the carpet plot. Lateral force computed from carpet plot is shown in Fig. 7, which is a function of slip angle at zero camber angle. Cornering stiffness is computed as follows:

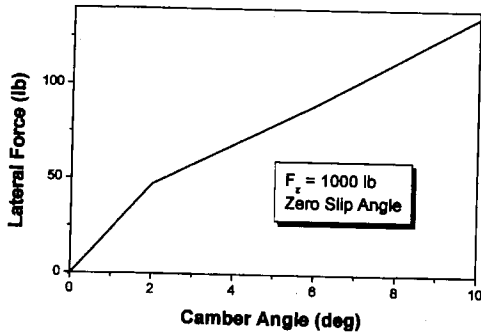


Fig. 8 Lateral force vs camber

$$C_{\alpha} = \left. \frac{dF_y}{d\alpha} \right|_{\alpha=0} = 50766.4 \quad (11)$$

Figure 8 shows lateral forces as a function of camber angle at zero slip with 1000lb of normal force. The Camber stiffness is computed as follows:

$$C_{\gamma} = \left. \frac{dF_y}{d\gamma} \right|_{\gamma=0} = 6011.4 \quad (12)$$

Road is assumed to be asphalt, so friction coefficient is assigned 0.85. Static and dynamic friction coefficients of AT_A model are 0.95 and 0.75, respectively.

3.3 Validation via simulation

The vehicle model employed in the simulation has a rack-pinion type steering system. The front suspension is a MacPherson strut type and the rear suspension is a twist axle with trailing arm. Vehicle has 25 d. o. f with 23 bodies, 28 joints, 4 bushings, and 4 TSDA (Translational-Spring-Damper-Actuator) elements.

3.3.1 Bump simulation

Bump simulation, frequently employed for a ride analysis, is performed at the speed of 48.8km/h. The vehicle meets half sine bump(its height is 10cm and length is 2m) 3 seconds after static equilibrium in vertical direction. The AT_A tire model is not compared here due to difficulty in road generation and the BASIC tire option is chosen in the AT_D model. Vertical positions and accelerations are shown in Fig. 9 and 10, respectively.

AT_S and AT_M tire models meet bump later

Table 2 CPU times for bump simulation

Tire Models	AT_C	AT_D	AT_M	AT_S
CPU time(sec)	31.755	31.81	32.23	31.038

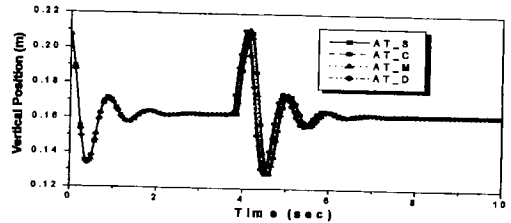


Fig. 9 Vertical positions of chassis

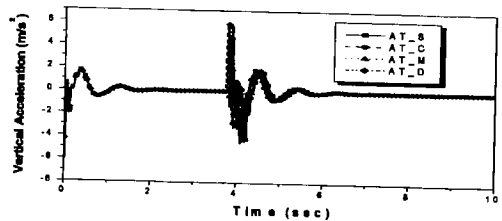


Fig. 10 Vertical accelerations of chassis

than other tire models, as shown in Fig. 9, because longitudinal force computed during static equilibrium reduces the velocity. The magnitudes and trend in vertical acceleration, however, are acceptable. For the bump simulation for 10 seconds of simulation times, CPU times are compared in Table 2.

3.3.2 Lane change maneuvers

Lane change maneuvers are simulated at the initial speed of 48.8km/h. The steering input is applied to rack bar 3 seconds after static equilibrium. Figures 11, 12 and 13 show the lateral position of vehicle, lateral acceleration and tire lateral force, respectively

Figure 13 shows that AT_D and AT_A models, which are theoretical models, are different from other models on lateral force. It can be explained by the fact that AT_D and AT_A tire models assume tire properties (cornering stiffness, camber stiffness and so on) constant. These parameters, however, are changeable according to tire normal force. The error of AT_M model may

Table 3 CPU times for lane change

Tire Models	AT_C	AT_D	AT_A	AT_M	AT_S
CPU time (sec)	31.624	31.759	37.856	31.04	31.887

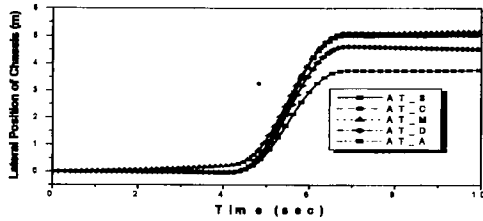


Fig. 11 Lateral position of chassis

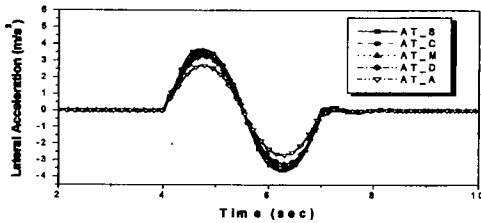


Fig. 12 Lateral accelerations of chassis

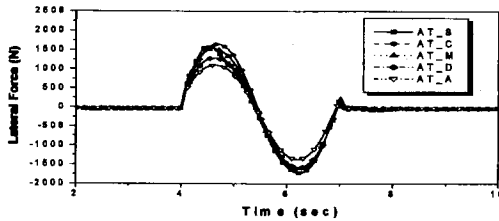


Fig. 13 Lateral forces of tire

results from curve fitting for its coefficients. For the lane change simulation for 12 seconds, CPU time is compared in Table 3.

3.3.3 Pulse steering simulation

AT_S tire model is selected as a reference model and the same steering input is applied to other tire models. Initial velocity was 80km/h, and the pulse shape is a half sine whose amplitude is adjusted to bound 0.4g of the maximum lateral acceleration. Lateral position of vehicle, yaw rate, and lateral acceleration are shown in

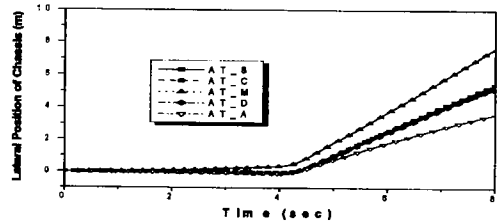


Fig. 14 Lateral position of chassis

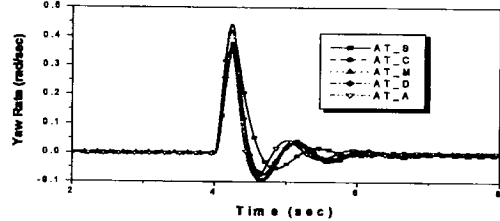


Fig. 15 Yaw rate of chassis

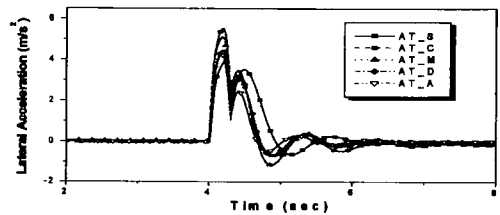


Fig. 16 Lateral acceleration of chassis

Figs. 14, 15 and 16, respectively. The performances are tested by four parameter evaluation method consisting of 4 parameters, i. e., steady state gain of yaw velocity response a_1 , natural frequency of yaw velocity response f_n , damping of yaw velocity ζ (zeta), and phase delay φ (phi) at 1Hz of lateral acceleration response. If a vehicle has a strong understeer (US) characteristic, the rhombus deflects to the right-higher direction. If a vehicle has a weak US characteristics, the rhombus deflects to the left-lower direction. Figure 17 shows rhombus by the post-processor of AutoDyn7.

The AT_C tire model is most different with others in Fig. 13 and 14 because the carpet plot data of AT_C model is measured at speed of 48.8km/h. Tire models except the AT_S model have shown understeer characteristics, as shown in Fig. 15. It can be explained that there are stronger understeer characteristics than the real phenome-

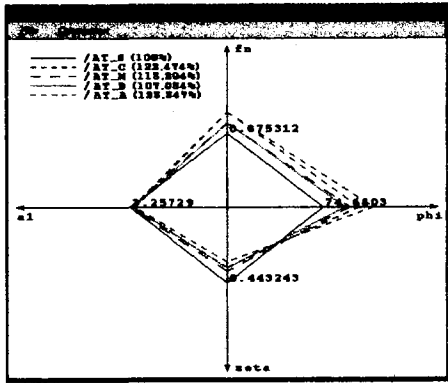


Fig. 17 Rhombus

Table 4 CPU times for step steer

Tire Models	AT_C	AT_D	AT_A	AT_M	AT_S
CPU time (sec)	26.824	26.842	26.781	30.54	27.35

non if any other tire models are used. For the pulse steering simulation of which simulation time is 12 seconds, CPU time is compared in Table 4.

4. Conclusion

Several tire models developed in the AutoDyn7 program are explained and compared.

Bump simulation gives almost the same results of vertical force for all tire models. The lane change maneuvers shows almost identical results for empirical tire models AT_S, AT_C, and AT_M. In the pulse steer simulation, empirical models AT_C and AT_M have a little difference, but AT_M tire model is better than AT_C tire model in understeer character.

From the comparison of several tire models, the following recommendations are obtained.

(1) For the bump simulations and, lane change maneuvers, any kinds of tire models can be used.

(2) For the pulse steer simulation, Magic formula model or STI Tire model are recommended.

Acknowledgement

This research are supported by the KOSEF (Project No. 97-0200-1001-5).

References

Bernard. J. E. Segel, L. and Wild, R. E., 1977, "Tire Shear Force Generation During Combined Steering and Braking Maneuvers," *SAE Transactions* 770852.

Choi, DaeHyung, 1999, "Derivation of the Coefficients of the MAGIC FORMULA from Carpet Plot and Simulation, Master's thesis, PNU.

Dugoff, H., 1977, "An Analysis of Tire Traction Properties Which May Influence of Vehicle Dynamic Performance," *SAE Transactions* 770377.

Fiala, E.,1954, "Seitenkräfte am Rollenden Luftreifen," *Z. VDI*, Vol. 96, No. 29.

Gim, Gwanghun, 1990, "An Analytical Model of Pneumatic Tyres for Vehicle Dynamic Simulations," *Int. J. of vehicle Design*, Vol. 1. No. 1.

Kim, KwangSuk, Yoo, WanSuk, Kim, SungSoo, Kim, SangSup, 1999, "Development of Vehicle Dynamics Program AutoDyn7()-Structure and Algorithm," *Transactions of KSAE*, Vol. 7, No. 3, pp. 321~330.

Lee, MinSeung, 1997, "Development UA tire model for vehicle dynamics program AutoDyn7," Master's thesis, PNU.

Mimuro, T., "Four Parameter Evaluation Method of Lateral Transient Response," *SAE paper*, 901734.

Pacejka, H. B., 1979, "Tyre Factors and Vehicle Handling," *Int. J. of vehicle Design*, Vol. 1. No. 1.

Salaani, Mohamed Kamel, 1996, "Development and Validation of a Vehicle Model for the National A Dvanced Driving Simulator," Ph. D, Ohio State Univ.

1997, DADS(Dynamic Analysis and Design System) User's Reference Manual, Computer Aided Design Software Inc.